The Journal of Experimental Biology **199**, 1029–1041 (1996)
Printed in Great Britain © The Company of Biologists Limited 1996
JEB0062

A COMPARTMENTAL APPROACH TO THE MECHANISM OF CALCIFICATION IN HERMATYPIC CORALS

ÉRIC TAMBUTTÉ[1,2], DENIS ALLEMAND[1,*], ERICH MUELLER[3,†] AND JEAN JAUBERT[1]

[1]*Observatoire Océanologique Européen (OOE), Centre Scientifique de Monaco, Avenue Saint Martin, MC 98000 Monaco, Principality of Monaco,* [2]*Commissariat à l'Énergie Atomique, Direction des Applications Militaires, Laboratoire de Géophysique, BP 12, F-91680 Bruyères-le-Châtel, France* and [3]*Department of Marine Sciences, University of South Alabama, Mobile, AL 36688, USA*

Accepted 11 January 1996

Summary

Ca^{2+} compartments, Ca^{2+} transport and the calcification process were studied by using ^{45}Ca as a tracer. The biological model used was clones of *Stylophora pistillata* developed into microcolonies whose skeleton is entirely covered by tissues, thus avoiding direct radioisotope exchange between the sea water and the skeleton. The study of Ca^{2+} compartments was performed by measuring two complementary parameters: Ca^{2+} influx and Ca^{2+} efflux kinetics. Kinetic analysis of ^{45}Ca uptake revealed three exchangeable and one non-exchangeable Ca^{2+} compartments in these microcolonies. The first compartment was saturable with a short half-time (4 min), correlated to external Ca^{2+} concentration and insensitive to metabolic or ion transport inhibitors. This compartment (72.88 nmol Ca^{2+} mg^{-1} protein) has been previously attributed to sea water present in the coelenteron. The second Ca^{2+} compartment (7.12 nmol Ca^{2+} mg^{-1} protein) was soluble in NaOH, saturable with a half-time of 20 min and displayed a combination of Michaelis–Menten kinetics and diffusional entry. It was insensitive to a variety of inhibitors but its loading was stimulated by Ca^{2+} channel inhibitors. On the basis of uptake experiments, the existence of a third compartment with a rapid turnover rate (about 2 min) and a very small size is predicted. It is suggested that this compartment corresponds to the calicoblastic epithelium. Ca^{2+} flux through this compartment was facilitated by voltage-dependent Ca^{2+} channels (with L-type characteristics) and Ca^{2+}-ATPase and was coupled to an anion carrier. Transcellular Ca^{2+} movement was dependent on the cytoskeleton. The rate of Ca^{2+} flux across this epithelium was about 975 pmol mg^{-1} protein min^{-1}. The fourth calcium compartment, corresponding to the skeleton, was soluble in HCl and non-exchangeable. After a short lag phase (about 2 min), the rate of Ca^{2+} deposition was linear over a period of at least 5 h. The calcification rate was 975 pmol mg^{-1} protein h^{-1} at an irradiance of 175 μmol photons m^{-2} s^{-1}. It followed Michaelis–Menten kinetics and saturated at levels (9 mmol l^{-1}) close to the Ca^{2+} concentration of sea water. Wash-out (efflux) experiments employing several different protocols allowed identification of six compartments. The first two compartments were extracellular (bulk extracolonial water and coelenteron). The third compartment may be part of the second Ca^{2+} compartment identified by influx experiments. A fourth compartment was sensitive to the Ca^{2+} channel inhibitor D600 and appeared to be associated with the NaOH-soluble (tissue) Ca^{2+} pool. Two compartments were identified during skeletal efflux, the first being small and due to either tissue carry-over or a labile skeletal compartment. The second compartment corresponded to bulk skeletal deposition. The various efflux protocols produced varying estimates of tissue Ca^{2+} levels and calcification rates and, thus, coral post-incubation processing has a profound impact on experimental interpretation.

Key words: scleractinian corals, *Stylophora pistillata*, calcification, Ca^{2+} transport, Ca^{2+} channel, kinetic analyses, carbonic anhydrase.

Introduction

Biocalcification is one of the most important biological process in the living world. Although an impressive amount of information has been produced in the last few years, calcification processes and, more specifically, the location and mechanism of Ca^{2+} transport largely remain a biological enigma (Wilbur and Simkiss, 1979; McConnaughey, 1989;

*Author for correspondence.
†Present address: Mote Marine Laboratory, Florida Keys Marine Research Center, PO Box 500895, Marathon, FL 30050 USA.

Simkiss and Wilbur, 1989; Cameron, 1990). It appears that there are two possible routes for Ca^{2+} transport during calcification: (1) paracellular, where ions pass through intercellular spaces and (2) transcellular. The paracellular pathway has been hypothesized to explain the diffusional entry in algae (Borowitzka, 1982) and the movement of Ca^{2+} across the mantle of molluscs (Wheeler, 1992), while transcellular movement has been suggested in corals (Barnes and Chalker, 1990) and crustaceans (Roer, 1980; Cameron, 1990).

One of the major calcifying groups of organisms is the scleractinian corals. The rate of calcification of a coral reef is assumed to be around $10\,kg\,CaCO_3\,m^{-2}\,year^{-1}$ (Chave *et al.* 1975). It has been calculated that, at peak calcification rate, cells of the calicoblastic epithelium of the fast-growing distal regions of the staghorn coral (*Acropora* sp.) must transport each hour all the calcium contained in 50–100 times their own volume (Gladfelter, 1984; Barnes and Chalker, 1990). In spite of this high flux of calcium, mechanisms of Ca^{2+} transport are still poorly understood and Ca^{2+} compartments in tissue have never been studied. Several lines of evidence indicate that calcification in corals depends upon a specific, energy-requiring transport mechanism (Chalker, 1976; Krishnaveni *et al.* 1989). The presence of a high-affinity Ca^{2+}-ATPase has been demonstrated (Isa *et al.* 1980; Ip *et al.* 1991). Carbonic anhydrase is also thought to control calcification rate (Silverton, 1991). However, kinetic studies of Ca^{2+} transport by coral tissues have been limited.

The main reason for this lack of data is the difficulty of using radioisotopes to study coral calcification. Buddemeier and Kinzie (1976) discussed the problems associated with the use of radioisotope techniques in the measurement of coral calcification. They identified the high variance of the results as the major experimental problem. This is due to isotopic exchange phenomena between ^{45}Ca in sea water and $CaCO_3$ in the porous aragonite skeleton during incubation (Clausen and Roth, 1975; Barnes and Crossland, 1977) and processing of samples after incubation (Crossland and Barnes, 1977). In order to overcome these problems, we have used cloned corals ('microcolonies') of the branching scleractinian coral *Stylophora pistillata* with no skeletal surfaces exposed to the radioisotope-labelled incubation medium and experimental protocols which enable us to obtain reproducible Ca^{2+} uptake measurements (Tambutté *et al.* 1995). These improvements have enabled us to demonstrate the presence of a large extracellular compartment in *S. pistillata*, which probably corresponds to the coelenteric cavity (Tambutté *et al.* 1995).

Kinetic analyses of Ca^{2+} influx and efflux have proved to be useful tools to study Ca^{2+} compartments in cell cultures (Borle, 1969*a*,*b*, 1990; Claret-Berthon *et al.* 1977) and in intact tissues (Van Breemen *et al.* 1979). In the present study, we used these two complementary procedures to characterize additional Ca^{2+} compartments within coral colonies and the movement of Ca^{2+} between them. The kinetic and pharmacological characteristics of these compartments are described here.

Materials and methods

Biological material

Microcolonies were propagated in the laboratory from small fragments of *Stylophora pistillata* collected at a depth of 5 m in front of the Marine Science Station, Gulf of Aqaba, Jordan. Colonies were packed in humidified plastic bags and transported to our laboratory (14 h transport time). Corals were stored in an aquarium (300 l) supplied with sea water from the Mediterranean Sea (exchange rate $2\,\%\,h^{-1}$), heated to 26±0.1 °C and illuminated with constant irradiance of $175\,\mu mol\,photons\,m^{-2}\,s^{-1}$ using metal halide lamps (Philips HQI-TS, 400 W) on a 12 h:12 h photoperiod. Microcolony propagation has been described by Tambutté *et al.* (1995). Briefly, terminal portions of branches (6–10 mm long) were cut from parent colonies and placed on a nylon net (1 mm×1 mm mesh) in the same conditions of light and temperature as parent colonies. After about 1 month, coral fragments became entirely covered with new tissues.

Determination of Ca^{2+} compartmentation

Two different protocols have been used to determine the kinetic characteristics of Ca^{2+} compartments in microcolonies. The first was based on uptake experiments. ^{45}Ca was measured in microcolonies after a 30 min wash-out of the coelenteric cavity. The second was based on efflux experiments, radioactivity being measured in the efflux medium.

Measurement of Ca^{2+} uptake and calcification rate

Measurements were made at equivalent times of day in order to avoid possible variation caused by endogenous circadian rhythms (Buddemeier and Kinzie, 1976). Microcolonies were placed in plastic holders and incubated for 5–300 min in beakers (6 ml) containing 240 kBq of ^{45}Ca (as $CaCl_2$, 1.38 MBq ml^{-1}, New England Nuclear) dissolved in sea water filtered using 0.45 μm Millipore membranes (FSW) as described by Tambutté *et al.* (1995). Water movement was maintained by magnetic stirring bars. Incubations of varying duration were carried out on at least three samples under light and temperature conditions similar to those described during culture. Samples (100 μl) of sea water were removed during each incubation for the determination of specific radioactivity.

At the end of the labelling period, each holder and its microcolony was immersed for 20 s in a beaker containing 600 ml of FSW, then rinsed five times with 5 ml of ice-cold glycine high-calcium medium ($50\,mmol\,l^{-1}$ $CaCl_2$, $950\,mmol\,l^{-1}$ glycine, pH adjusted to 8.2) to prevent further Ca^{2+} uptake and to reduce, by isotopic dilution, the ^{45}Ca adsorbed onto the external surface of both the microcolony and the holder. The total duration of the rinsing procedure was less than 1 min. Labelled microcolonies were then put in a beaker containing 20 ml of FSW for 30 min to monitor ^{45}Ca efflux. The total amount of radioisotope released into the FSW was used to determine the size of the coelenteric cavity (Tambutté *et al.* 1995). Upon completion of the efflux procedure, microcolony tissues were dissolved completely over a period of 20 min in 1 ml of $2\,mol\,l^{-1}$ NaOH at 90 °C. The supernatant

(hereafter termed the 'NaOH-soluble pool') was collected and the skeleton was rinsed first in 1 ml of distilled water and, subsequently, five times in 5 ml of FSW. The first rinse solution was added to the NaOH pool, the remaining five washes were discarded since they did not contain proteins. Finally, the skeletons were dried and dissolved in 1.5 ml of 12 mol l^{-1} HCl overnight ('HCl-soluble pool'). Radioactive samples were added to 4 ml of Luma-gel (Packard) after neutralization and β emissions measured using a liquid scintillation counter (Tricarb, 1600 CA Packard).

Measurement of calcification rate in short incubations

In order to determine the calcification rate during short incubations, the rinsing procedure was bypassed by using EGTA. At the end of the labelling period, and after a short immersion in 600 ml of FSW, the microcolony was immediately immersed for 30 min in 10 ml of 5 mmol l^{-1} EGTA in 1 mol l^{-1} NaOH in order to chelate Ca^{2+} absorbed by the coelenteron and the tissues. After this treatment, the microcolony was processed as described above.

Ca^{2+} efflux

Microcolonies were incubated with ^{45}Ca for 3 h at 25 °C under an irradiance of 675 μmol photons m^{-2} s^{-1}. Colonies were then transferred to one of the three efflux media, Ca^{2+}-free artificial sea water ($0Ca^{2+}$/ASW), $0Ca^{2+}$/ASW with 5 mmol l^{-1} EGTA ($0Ca^{2+}$/EGTA) or FSW. Effluxes into $0Ca^{2+}$/EGTA and FSW were conducted either on ice or at 25 °C. Efflux into $0Ca^{2+}$/ASW was on ice only. Efflux was performed by sequential incubations of microcolonies at increasing intervals over 180 min into beakers containing 20 ml of medium. Tissues were then removed as described above, the remaining skeletons were returned to efflux medium and transferred in a manner similar to the intact microcolonies. Skeletons were dissolved as described previously. Samples of all efflux solutions and the NaOH and HCl pools were counted in a liquid scintillation counter.

Media and chemicals

For experiments with varying Ca^{2+} concentrations, ASW was prepared from distilled water according to the method of Allemand *et al.* (1984). $CaCl_2$ was replaced by NaCl in order to maintain constant osmolarity. DIDS (4,4′-diisothiocyanatostilbene-2,2′-disulphonic acid), (+)-verapamil, (−)-verapamil, (+)-methoxyverapamil or (−)-D600, (−)-methoxyverapamil or (+)-D600, diltiazem, ethoxyzolamide, thapsigargin, cytochalasin B, colchicine and Bay K 8644 were dissolved in DMSO (dimethyl sulphoxide). Cadmium chloride, nickel chloride, NaCN and ω-conotoxin were dissolved in water. Nifedipine was dissolved in acetone. Lanthanum chloride was dissolved in ethanol; flunarizine was dissolved in methanol. The final solvent concentration was never more than 1% (v/v). Preliminary experiments showed that this concentration had no effect on Ca^{2+} uptake (results not shown). Except for (−)-verapamil, (−)-D600 and Bay K 8644 (generous gift from Dr Barhanin), all chemicals were obtained from Sigma and were of analytical grade. When inhibitors were used, a 15 min pre-incubation step was included. The inhibitor was continuously present at the same concentration during pre-incubation, incubation (1 h) and efflux (30 min) periods.

Protein concentrations were measured using the method of Lowry *et al.* (1951) in an autoanalyzer (Alliance Instruments) using bovine serum albumin as the standard. Results are expressed as nmol Ca^{2+} mg^{-1} protein in the NaOH-soluble pool (milligrams of protein per microcolony) and represent means ± S.D. for at least three measurements.

Statistical analyses and curve fitting

Curve fitting of uptake experiments was performed using the Igor wave metrics program with either the exponential ($y=k_0+k_1e^{-k_2x}$) or linear ($y=k_0+k_1x$) equations. Results are presented as means of at least three points ± S.D. Student's *t*-test was used to evaluate differences between means. Differences with $P<0.05$ were taken as significant. The half-time ($t_{1/2}$) of compartment loading was either calculated graphically from a semi-logarithmic plot of the data according to the following equation:

$$\ln(Q_{eq}-Q) = \ln Q_{eq} - kt, \quad (1)$$

in which the slope was the rate constant, k, or from:

$$t_{1/2} = (\ln 2)/k, \quad (2)$$

where Q_{eq} is the total quantity of radioactivity in the compartment at equilibrium, and Q is the total quantity of radioactivity at each sampling time t. The flux towards a given compartment was given by the equation:

$$\text{unidirectional flux} = k(\text{compartment size}) \quad (3)$$

(Borle, 1990).

Efflux curves were constructed by sequentially adding effluxed Ca^{2+} to that remaining in the HCl- (skeletal) and NaOH- (tissue) soluble pools. The resulting efflux curves were then graphically 'peeled' into linear components (semi-logarithmic plot) and fitted using the graphics program DeltaGraph. The efflux curves were modelled using a general exponential equation:

$$[Ca^{2+}]_o = \sum[Ca^{2+}]_n(e^{-kt}), \quad (4)$$

where $[Ca^{2+}]_o$ is the calcium concentration at the beginning of the efflux period, $[Ca^{2+}]_n$ is the calcium concentration in compartment n, k is the rate constant and t is the time. The $t_{1/2}$ for each component was calculated as $(\ln 2)/k$.

Results

Time course of Ca^{2+} uptake and deposition

The rates of Ca^{2+} uptake by the coelenteric compartment, the NaOH-soluble pool and the HCl-soluble pool are depicted in Fig. 1. Ca^{2+} uptake by both the coelenteric compartment and the NaOH-soluble pool displayed saturable kinetics (Fig. 1A,B). Isotopic equilibrium was reached at about 10 min and

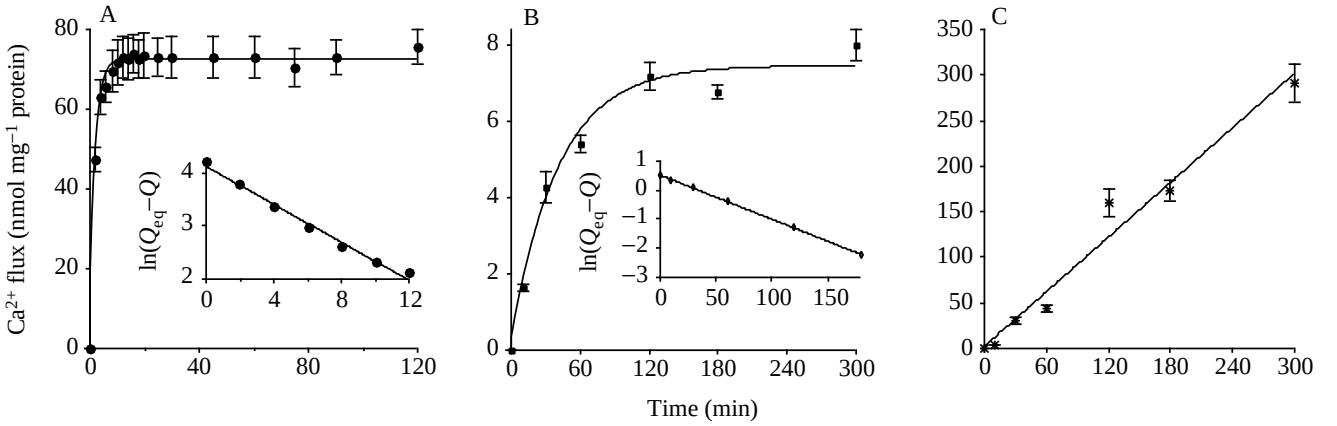

Fig. 1. Time course of Ca^{2+} fluxes in (A) the coelenteric compartment, (B) the NaOH- and (C) the HCl-soluble Ca^{2+} pools. Measurements for the coelenteric compartment were obtained from efflux experiments in FSW (see Materials and methods). The time courses of NaOH- and HCl-pool loading were obtained by direct measurement of ^{45}Ca uptake. Insets: semi-logarithmic plots for the determination of $t_{1/2}$. Values are means ± S.D., N=5.

2 h in the coelenteron and in the NaOH-soluble compartment respectively. The equilibrium value corresponds to the size of the exchangeable Ca^{2+} compartment, i.e. 72.88±1.35 nmol Ca^{2+} mg^{-1} protein for the coelenteric compartment and 7.12±0.72 nmol mg^{-1} protein for the NaOH-soluble pool. The half-times of exchange ($t_{1/2}$) of these compartments, are, respectively, 4 and 20 min as determined by semi-logarithmic treatment of the data (insets of Fig. 1A,B). From the value of $t_{1/2}$, the respective rate constants can be calculated to be 0.17 and 0.034 min^{-1}. The initial rate of Ca^{2+} flux is obtained from the product of compartment size and k. The value determined for the initial rate of Ca^{2+} flux from sea water into the coelenteric compartment is therefore 12 629 pmol mg^{-1} protein min^{-1}, and that from sea water (and the coelenteric compartment) into the NaOH-soluble pool is 224 pmol mg^{-1} protein min^{-1} (Table 1).

The time course of Ca^{2+} deposition in the skeletal compartment (HCl-soluble pool) was linear until at least 5 h (Fig. 1C). No lag phase could be detected under our experimental conditions. The calcification rate appears to be 975 pmol mg^{-1} protein min^{-1}. In order to study the onset of Ca^{2+} deposition into the skeleton, we performed short-term

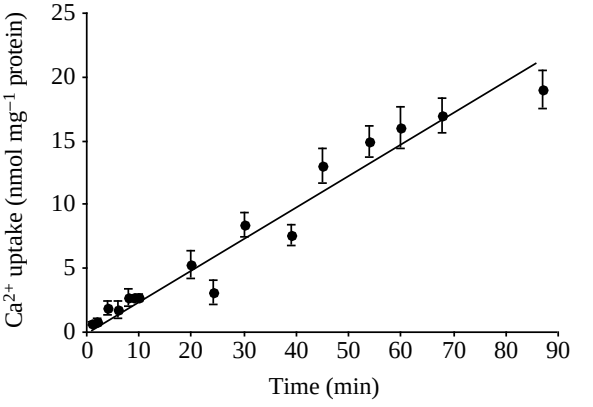

Fig. 2. Kinetics of ^{45}Ca incorporation into the HCl-soluble pool over a short time period. Values are means ± S.D., N=3.

Table 1. *The calcium compartments in* Stylophora pistillata *microcolonies as characterized by uptake experiments*

Pool	$t_{1/2}$ (min)	Pool size (nmol Ca^{2+} mg^{-1} protein)	Fluxes (pmol mg^{-1} protein min^{-1})	Anatomical correlate
(1) Efflux	4	72.9	12 629 (with sea water)	Coelenteron
(2) NaOH-soluble	20	7.12	224 (with sea water and 1)	Tissue except calicoblastic epithelium
(3) Hypothetical	<2	?	975 (with 1 and 2)	Calicoblastic cells
(4) HCl-soluble	–	Infinite	975 (with 3)	Skeleton

$t_{1/2}$, half-time of compartment loading.

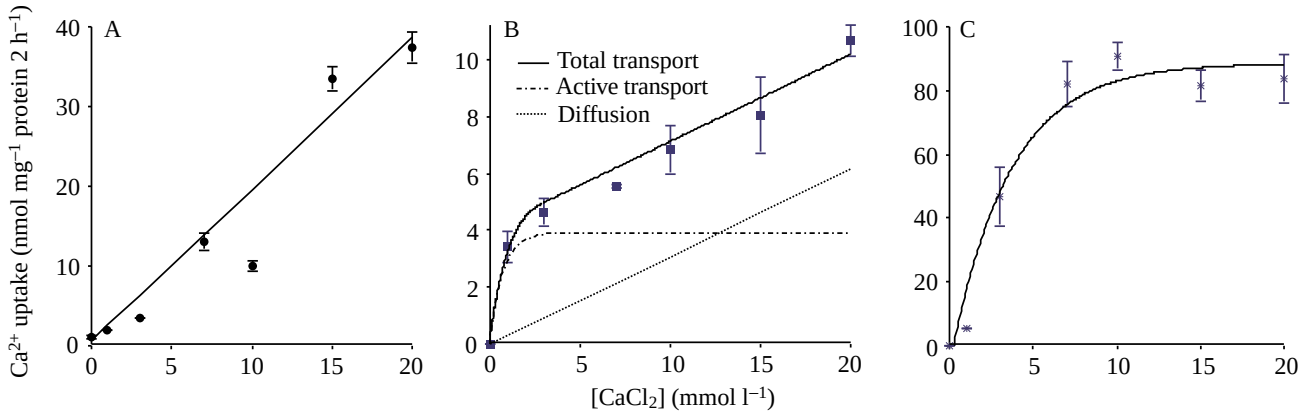

Fig. 3. Concentration-dependence of Ca^{2+} uptake by (A) the coelenteric compartment, (B) the NaOH- and (C) the HCl-soluble Ca^{2+} pools. Ca^{2+} uptake is plotted against the Ca^{2+} concentration in the sea water. In B, the total flux (experimental data, solid line) is broken into its two components, one saturable, describing a carrier-mediated transport system (dot-dashed line), and the other diffusional (dotted line). Values are means ± S.D., *N*=4.

incubations from 1 to 90 min. This procedure does not allow us to determine Ca^{2+} uptake by coelenteron and tissue. It can be seen in Fig. 2 that ^{45}Ca incorporation into the skeleton starts after a very short lag phase of less than 2 min and remains linear over the time range studied.

Effects of substrate concentration

Fig. 3 shows ^{45}Ca uptake at various external Ca^{2+} concentrations ranging from 0 to 20 mmol l^{-1}. While Ca^{2+} uptake by the coelenteric compartment is linearly correlated to the external Ca^{2+} concentration (Fig. 3A), uptake into the NaOH-soluble pool displays biphasic kinetics (Fig. 3B). The Ca^{2+} uptake is curvilinear at low Ca^{2+} concentrations (below 4 mmol l^{-1}) and becomes linear at higher values. Over the entire substrate concentration range, calcium uptake follows a combination of Michaelis–Menten kinetics plus an apparent adsorption or more likely a diffusional component, since microcolonies had been rinsed in a high-calcium medium to remove unspecific labelling by isotopic dilution. By subtracting the apparent diffusion (determined as a regression line parallel to the total flux of Ca^{2+} between 5 and 20 mmol l^{-1}) from the total uptake, the flux can be broken into two components. Ca^{2+} deposition in coral skeleton showed typical saturable Michaelis–Menten kinetics, the plateau being reached at about 9 mmol l^{-1} (Fig. 3C). These results support the view that a transport system for Ca^{2+} is involved in at least one step of the biocalcification mechanism.

Pharmacology

In order to characterize the three Ca^{2+} compartments

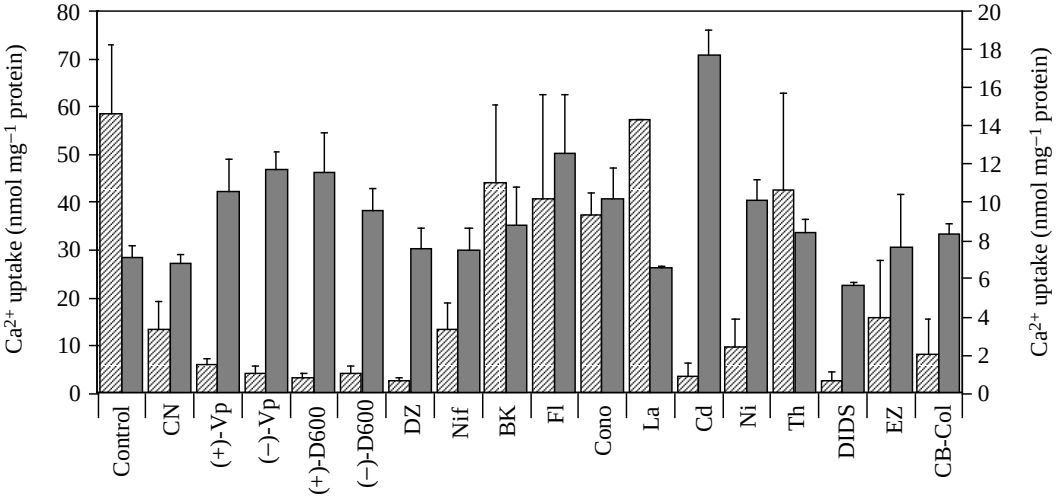

Fig. 4. Pharmacological characteristics of the NaOH- (filled bars; right-hand axis) and HCl- (hatched bars; left-hand axis) soluble Ca^{2+} pools. Effect of a metabolic inhibitor (1 mmol l^{-1} NaCN, CN), Ca^{2+} channel inhibitors [100 μmol l^{-1} (+)- and (−)-verapamil, Vp; 100 μmol l^{-1} (+)-D600 and (−)-D600; 100 μmol l^{-1} diltiazem, DZ; 100 μmol l^{-1} nifedipine, Nif; 10 μmol l^{-1} Bay K 8644, BK; 100 μmol l^{-1} flunarizine, Fl; 2 μmol l^{-1} ω-conotoxin, Cono] heavy metals (200 μmol l^{-1} lanthanum, La; 1 mmol l^{-1} cadmium, Cd; or nickel, Ni), an endoplasmic reticulum Ca^{2+}-ATPase inhibitor (5 μmol l^{-1} thapsigargin, Th), an anion transport inhibitor (300 μmol l^{-1} DIDS), a carbonic anhydrase inhibitor (300 μmol l^{-1} ethoxyzolamide, EZ) and inhibitors of microtubule and microfilament polymerization (250 μmol l^{-1} colchicine and 20 μmol l^{-1} cytochalasin B, CB-Col). ^{45}Ca uptake lasted for 1 h. Results are expressed as nmol Ca^{2+} mg^{-1} protein and values are means + S.D., *N*=3.

identified by uptake experiments and to determine the ion transport mechanism, we tested the effects of different drugs known for their ability to inhibit specific metabolic or transport mechanisms. The coelenteric compartment has previously been described as being insensitive to inhibitors of cell metabolism and ion transport (Tambutté *et al.* 1995). In the presence of 1 mmol l^{-1} sodium cyanide, a well-known mitochondrial inhibitor, Ca^{2+} uptake by the NaOH-soluble pool was unchanged (*t*-test, $P>0.05$), whereas Ca^{2+} deposition in skeletal structures was inhibited (Fig. 4) (*t*-test, $P<0.05$). The inhibition of Ca^{2+} deposition demonstrates that the formation of calcium carbonate is an energy-requiring process.

To test whether Ca^{2+} uptake was through voltage-dependent Ca^{2+} channels, we tested the effect of organic Ca^{2+} channel inhibitors [100 μmol l^{-1} (+)- and (−)-verapamil, (+)- and (−)-D600, diltiazem, nifedipine, 100 μmol l^{-1} flunarizine, 2 μmol l^{-1} ω-conotoxin] or heavy metals (200 μmol l^{-1} lanthanum, 1 mmol l^{-1} cadmium or nickel). Fig. 4 shows that most of these drugs stimulated by a factor of 1.2–2 the Ca^{2+} loading of the NaOH-soluble pool, whereas Ca^{2+} deposition in the HCl-soluble pool was almost entirely inhibited (*t*-test, $P<0.05$) except by ω-conotoxin, flunarizine and lanthanum. No differences were found between the effects of the stereoisomers of verapamil and D600. A dose–response experiment was performed with (+)-verapamil. Half-maximal inhibition was obtained for a verapamil concentration of 16 μmol l^{-1} (Fig. 5). Surprisingly, Bay K 8644, a Ca^{2+} channel agonist (Spedding and Paoletti, 1992), had no significant effect on Ca^{2+} uptake (*t*-test, $P>0.05$).

We also tested DIDS, an inhibitor of anion transport systems (Cabantchik and Greger, 1992), and thapsigargin, an inhibitor of endoplasmic reticulum Ca^{2+} uptake (Wictome *et al.* 1992).

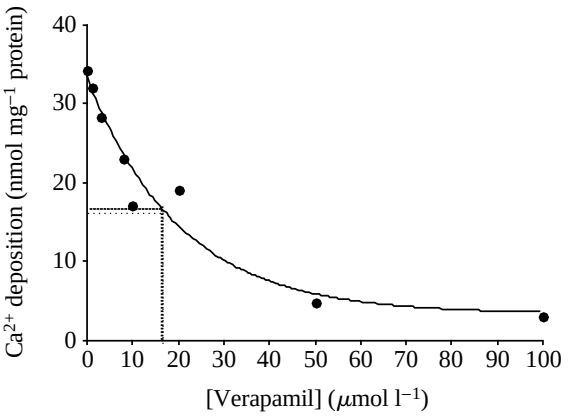

Fig. 5. Dose–response relationship for the effect of (+)-verapamil on ^{45}Ca skeletal deposition (HCl-soluble pool) during 1 h of incubation. IC_{50} for verapamil is 16 μmol l^{-1}.

It can be seen in Fig. 4 that 300 μmol l^{-1} DIDS greatly inhibited Ca^{2+} deposition in the HCl-soluble pool (*t*-test, $P<0.05$) but had no effect on the loading of the NaOH-soluble Ca^{2+} pool (*t*-test, $P>0.05$). Thapsigargin (5 μmol l^{-1}) had no effect on either pool (*t* -test, $P>0.05$).

The effect of the carbonic anhydrase inhibitor ethoxyzolamide (300 μmol l^{-1}) was investigated. This drug did not affect the uptake of Ca^{2+} by the NaOH-soluble pool (*t*-test, $P>0.05$) but inhibited Ca^{2+} deposition in the skeleton (*t*-test, $P<0.05$). Finally, we tested the effect of inhibitors of microtubule and microfilament polymerization, colchicine (250 μmol l^{-1}) and cytochalasin B (20 μmol l^{-1}). A mixture of these drugs had no significant effect on the NaOH-soluble pool (*t*-test, $P>0.05$), but prevented Ca^{2+} incorporation into the skeleton (*t*-test, $P<0.05$).

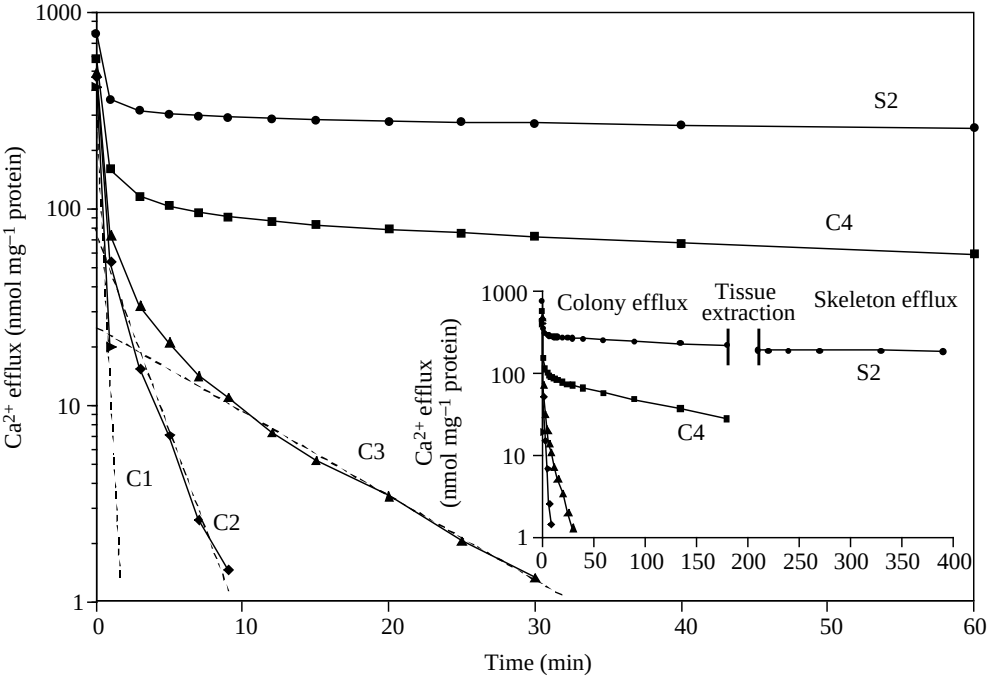

Fig. 6. Detail of a typical experiment showing the first 60 min of efflux of ^{45}Ca from four microcolonies in ice-cold 0Ca/ASW after 3 h of incubation at 25 °C with an irradiance of 675 μmol photons m^{-2} s^{-1}. Solid lines connect data points obtained by adding Ca^{2+} lost in each efflux interval and during tissue extraction back to the Ca^{2+} remaining in the skeleton (HCl pool). Compartment curves [C1, C2, C3, C4, S1 (not shown) and S2] were derived by sequentially removing mono-exponential components and are shown as dashed lines. Inset shows 400 min efflux of ^{45}Ca.

Table 2. *Compartments identified by colony (C) and skeletal (S) components under various efflux conditions*

Temperature (°C)	Medium	C1		C2		C3		C4		S1		S2	
		$t_{1/2}$	Ca^{2+}	$t_{1/2}$	Ca^{2+}	$t_{1/2}$	Ca^{2+}	$t_{1/2}$	Ca^{2+}	$t_{1/2}$	Ca^{2+}	$t_{1/2}$	Ca^{2+}
<1	0Ca/EGTA	13.2	273.4	2.9	52.6	28.3	18.6	76.1	138.9	19.6	12.6	1949	86.8
25	0Ca/EGTA	17.9	236.7	2.1	46.2	16.4	42.2	72.5	125.0	9.9	13.3	1114	83.3
<1	FSW	14.6	539.7	2.5	74.4	14.5	20.4	741.7	33.1	6.9	2.1	10169	264.5
25	FSW	13.9	352.2	2.1	56.7	10.3	8.6	691.9	6.5	12.9	1.4	10013	168.8
<1	0Ca/ASW	13.6	419.9	1.7	50.3	7.2	22.3	115.0	86.5	1.3	1.8	5159	198.7

The values for $t_{1/2}$ are in minutes except those in the column under C1, which are in seconds.
Compartment sizes (Ca^{2+}) are in nmol Ca^{2+} mg^{-1} protein.
All values were derived from pooled data representing four microcolonies.
$t_{1/2}$, half-time for Ca^{2+} efflux; FSW, filtered sea water; details of other media are given in Materials and methods.

Efflux protocols

A typical 400 min efflux curve is shown in the inset of Fig. 6. The data points (solid line) were obtained by sequentially adding back ^{45}Ca lost in the efflux solutions and NaOH-soluble pool to that remaining in the skeleton (HCl-soluble pool). The efflux curve was then 'peeled' by removing exponential components starting with the S2 (skeletal) compartment. A small S1 compartment (results not shown) was detected during the first few minutes of skeleton efflux. The colony (C) compartments are characterized after subtracting the S2 compartment. Fig. 6 shows the first 60 min of colony efflux to show the resolution of the C1 to C4 compartments. The values for $t_{1/2}$ and the sizes of each compartment are presented in Table 2 as measured under various efflux conditions. It should be noted that the $t_{1/2}$ values do not necessarily represent those of relevant physiological processes; they are used primarily to identify compartments. The C1 compartment has been associated with extracolonial water carried over on the plastic holders and on the outside of the colony. Similar rate constants were obtained with the holders alone (data not shown). The $t_{1/2}$ values for C1 were very similar for the different efflux conditions, averaging 14.6±1.9 s (mean ± S.D., N=4). The size of the C1 compartment varied, although this probably had little physiological significance. The C2 compartment had similar $t_{1/2}$ values (2.3±0.46 min) and also a similar size (56.0±10.9 nmol Ca^{2+} mg^{-1} protein) regardless of efflux conditions. The rate constants were slightly higher (lower $t_{1/2}$ values) at 25 °C, consistent with the effect of temperature on diffusion. This compartment is thought to be coelenteric; it was insensitive to D600 (data not shown) and had a size consistent with that determined by uptake kinetics (62.5 nmol Ca^{2+} mg^{-1} protein; see above). The C3 compartment was also insensitive to D600 and its size and time constant did not vary widely with efflux conditions. Again, rate constants were slightly higher at 25 °C; the mean value of $t_{1/2}$ was 15.3±8.1 min. The compartment size varied from 8.6 to 42.2 nmol Ca^{2+} mg^{-1} protein.

The size of the C4 compartment was sensitive to 10 μmol l^{-1} D600 (Fig. 7) and this compartment showed substantial variation in both rate constant and size depending upon the efflux conditions. In ice-cold 0Ca/EGTA, $t_{1/2}$ was 76.1 min; it was only slightly shorter at 25 °C (72.5 min). The size of this compartment was similar, around 130 nmol Ca^{2+} mg^{-1} protein, in this medium at 0 °C and 25 °C. Elimination of EGTA decreased the rate constant and size of the C4 compartment: in FSW, $t_{1/2}$ values of hundreds of minutes were obtained and compartment size was much smaller. To determine whether the C4 compartment corresponded to the intracellular pool, its size was calculated at the time when tissue Ca^{2+} depletion was initiated (or the end of colony efflux; $C4_{180}$) and compared with the size of the NaOH-soluble pool (Table 3). The NaOH-soluble pool was always smaller than $C4_{180}$. The discrepancy was smallest when 0Ca/ASW was used as the efflux medium.

The skeletal effluxes yielded two components, a small, relatively fast S1 compartment and a larger, much slower S2 compartment. The $t_{1/2}$ value of S1 generally varied from 7 to

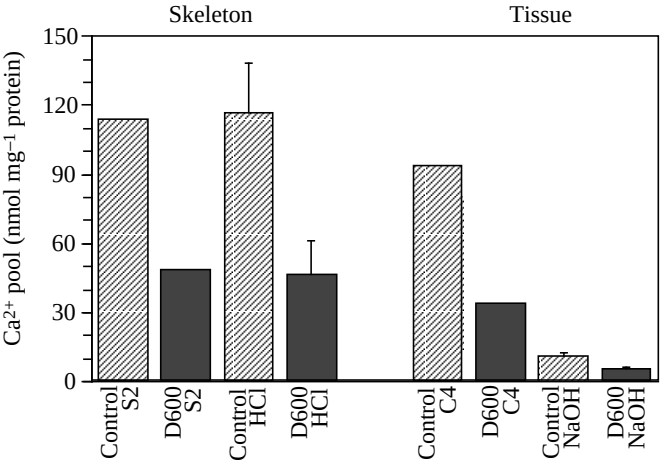

Fig. 7. Comparison of the sizes of tissue (C4, NaOH) and skeletal (S2, HCl) Ca^{2+} pools in the presence and absence of 10 μmol l^{-1} D600. Colonies were incubated for 3 h in the presence of D600 at 25 °C with an irradiance of 675 μmol photons m^{-2} s^{-1}. Efflux medium was ice-cold artificial sea water with 0Ca^{2+}/EGTA. Values are derived from pooled efflux curves representing four microcolonies (means + S.D.). The effect of D600 is significant at the P<0.01 level for both the HCl- and NaOH-soluble pools (t-test).

Table 3. *Comparison of the calculated C4 compartment Ca^{2+} content after the efflux procedure ($C4_{180}$) with the Ca^{2+} content of the NaOH-soluble pool under various efflux conditions*

Temperature (°C)	Medium	$C4_0$	$C4_{180}$	NaOH-soluble pool	
				Mean	S.D.
<1	0Ca/EGTA	138.9	26.95	15.32	1.78
25	0Ca/EGTA	125	22.36	9.92	0.5
<1	FSW	33.1	33.07	26.47	10.7
25	FSW	6.5	7.78	6.6	1.8
<1	0Ca/ASW	86.5	29.23	28.1	6.2

Calculated C4 Ca^{2+} content at the beginning of the efflux period ($C4_0$, data from Table 2) is also shown.

All values are expressed as nmol Ca^{2+} mg^{-1} protein and are derived from four replicate microcolonies.

Details of media are given in Materials and methods.

20 min: however, it was 1.3 min in 0Ca/ASW (Table 2). In the presence of EGTA, the compartment was larger (approximately 13 nmol Ca^{2+} mg^{-1} protein) compared with that in media without EGTA (1.8±0.4 nmol Ca^{2+} mg^{-1} protein). The S2 compartment also showed an effect of EGTA. When in the efflux medium, the $t_{1/2}$ value was shorter and the size smaller compared with these values in FSW. Although the rate constants were similar, the compartment size in FSW was smaller at 25 °C. The 0Ca/ASW medium produced an S2 component that had an intermediate rate constant and a size more similar to those obtained in FSW. In Fig. 7, it can be seen that the S2 compartment corresponds well with the HCl-soluble pool.

Effect of D600 on efflux compartments

Using the 0Ca/EGTA efflux protocol, the effects of 10 μmol l^{-1} D600 on the sizes of the NaOH- and HCl-soluble pools and their putative compartmental analogues were compared. D600 inhibited uptake into the S2 and HCl-soluble compartments by approximately 60 %; the absolute values of the pool sizes are also in close agreement (Fig. 7). The C4 Ca^{2+} content (at time=0) was much higher than that of the NaOH-soluble pool, but both were D600-sensitive. C4 Ca^{2+} efflux was inhibited by 64.2 % while efflux from the NaOH-soluble pool was inhibited by 49.0 %.

Discussion

Mechanism of ion transport for calcification

The Ca^{2+} transport mechanism of calcifying systems has received relatively little attention (Wilbur, 1976; Simkiss and Wilbur, 1989; Neufeld and Cameron, 1994). In scleractinian corals, most authors have focused their research on Ca^{2+} incorporation into the skeleton without studying calcium homeostasis in tissue. The present study shows that calcium reaches the site of calcification by an energy-requiring process through a transcellular pathway (see Fig. 8). Skeletal Ca^{2+} deposition displays saturable kinetics with respect to the calcium concentration in sea water, implying a carrier-mediated step. This result confirms a previous report (Chalker, 1976) suggesting an intracellular pathway for Ca^{2+} transport in corals, differentiating this mechanism from those found in the posterior caecum of the amphipod *Orchestia cavimana* (Meyran *et al.* 1984) or mollusc mantle (Wheeler, 1992).

Calcification is inhibited by organic or inorganic Ca^{2+} channel inhibitors (Figs 4, 5), as previously hypothesized (Mueller, 1984). The presence of voltage-dependent Ca^{2+} channels has been demonstrated in numerous marine invertebrates (Adams and Gage, 1979; Schmidt *et al.* 1982; Bilbaut *et al.* 1988) but the involvement of these channels in biocalcification has been demonstrated in only a few calcifying organisms such as echinoids (see review by Dubois and Chen, 1989) and red coral (Allemand and Grillo, 1992). Our present results show that such Ca^{2+} channels are also present in scleractinian corals and are responsible for the passive entry of Ca^{2+} into cells through which the bulk, if not all, of the skeletal Ca^{2+} must pass.

From pharmacological data, it appears that ^{45}Ca deposition into the skeleton is highly sensitive (inhibition greater than 90 %; IC_{50} for verapamil of 16 μmol l^{-1}) to both stereoisomers of phenylalkylamines (verapamil and D600) and to benzothiazepines (diltiazem). Dihydropyridine (nifedipine) is also a very potent inhibitor (inhibition of about 80 %). In contrast, calcification is only weakly sensitive to typical inhibitors of N channels (ω-conotoxin) or T channels (flunarizine). This sensitivity pattern suggests that Ca^{2+} transport for calcification is performed by a Ca^{2+} channel whose pharmacological characteristics are close to those of the L-type of voltage-sensitive Ca^{2+} channel described in mammalian cells (Hosey and Lazdunski, 1988; Spedding and Paoletti, 1992). Because they display a prolonged opening time, Ca^{2+} channels of this type appear to be involved primarily in the regulation of intracellular Ca^{2+} homeostasis in a wide range of tissue including non-excitable cells (Miller and Fox, 1990; Pietrobon *et al.* 1990). The higher sensitivity to cadmium in comparison with nickel is also in agreement with this conclusion (Miller and Fox, 1990). Surprisingly, lanthanum did not affect calcification. Lanthanum-insensitive Ca^{2+} channels have also been described in fish (Marshall *et al.* 1992). Further studies are planned in order to characterize better the Ca^{2+} channel involved in calcification.

These data demonstrate that Ca^{2+} uptake by coral tissue is an obligatory step in skeleton formation. This conclusion contradicts the hypothesis of Johnston (1980), who proposed that Ca^{2+} was transported by vesicles *via* a paracellular route. This author suggested that the zonular cell junctions present between calicoblastic cells are dynamic structures that may open and re-form to allow passage of Ca^{2+}-containing vesicles into the subcalicoblastic space. The absence of a diffusional component argues strongly against any continuity, even temporary, between the coelenteric fluid and the calcification site (Fig. 3C).

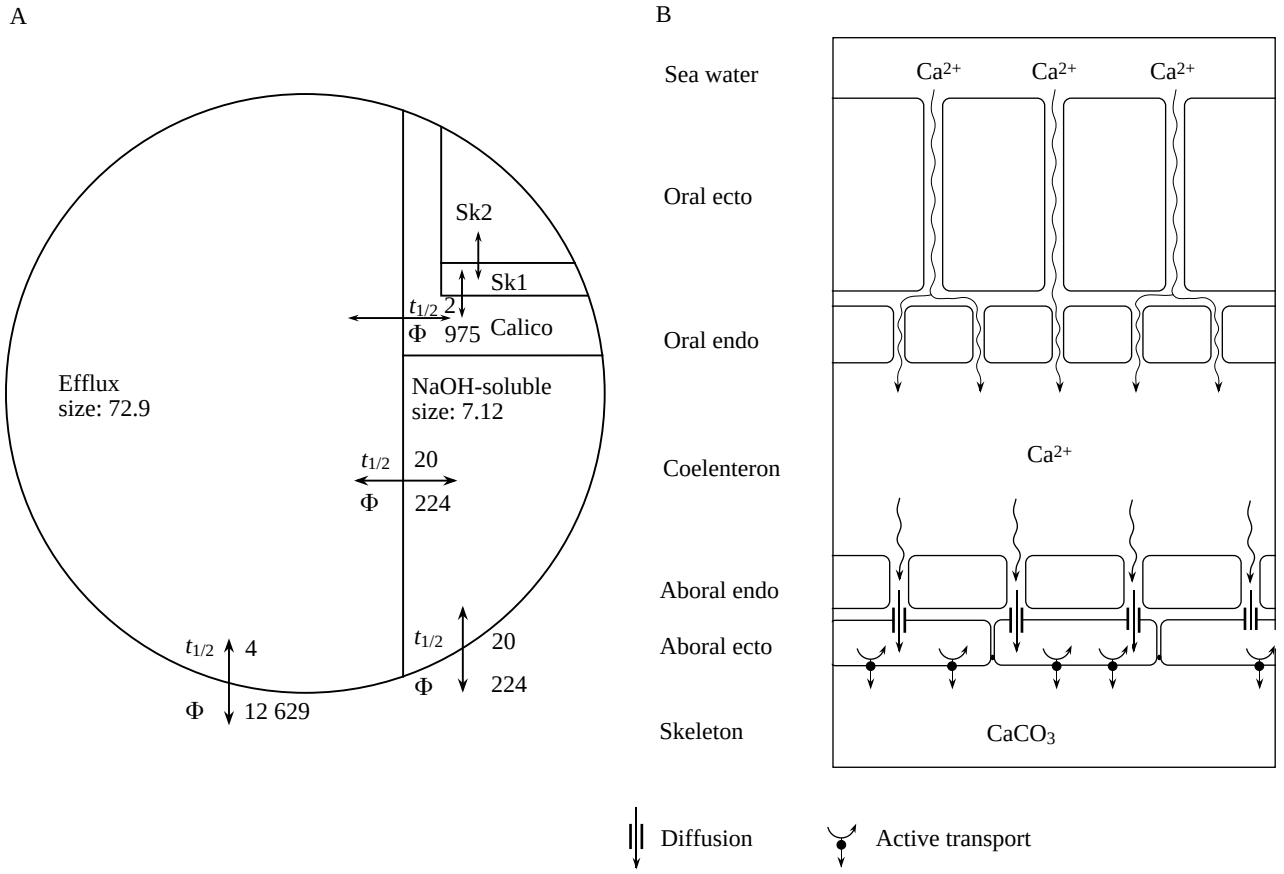

Fig. 8. Model of distribution and exchange rates of Ca^{2+} in a *Stylophora pistillata* microcolony. (A) Theoretical model. Exchange rates (Φ, in pmol mg^{-1} protein min^{-1}), half-times ($t_{1/2}$, in min) and compartment sizes (in nmol mg^{-1} protein) are presented (as determined from influx experiments). The efflux compartment should correspond to the coelenteron. The tissue compartment should be composed of the NaOH-soluble pool measured using influx experiments and possibly corresponding to C3, and a hypothetical compartment of very small size corresponding to the calcifying compartment (calicoblastic epithelium: Calico). The skeletal compartment should be composed of two calcium pools: a small labile skeletal pool (Sk1) and the bulk skeleton (Sk2). (B) Anatomical interpretation. The figure shows the two epithelial cell layers, the oral ectoderm (Oral ecto) and endoderm (Oral endo) and the aboral endoderm (Aboral endo) and ectoderm (Aboral ecto).

The transcellular movement of Ca^{2+} could be performed by transport *via* intracellular vesicles and their subsequent discharge at the mineralizing front (Hayes and Goreau, 1977; Johnston, 1980) or by Ca^{2+}-binding proteins (Simkiss, 1976; Bronner, 1990). The insensitivity of the calcification process to thapsigargin, a specific inhibitor of the Ca^{2+}-ATPase that is thought to load intracellular Ca^{2+} stores (Wictome *et al.* 1992), suggests that transcellular transport of Ca^{2+} is not achieved by intracellular vesicles. Furthermore, the sensitivity to Ca^{2+} channel inhibitors rules out the hypothesis that pinocytic vacuoles transport Ca^{2+}. The presence of Ca^{2+}-binding proteins as bulk intracellular carriers (Bronner, 1990) remains a viable hypothesis. Experiments are under way to address this point.

The anion carrier inhibitor DIDS was also a strong inhibitor of calcification. A similar finding was reported for spicule formation in echinoids by Mitsunaga *et al.* (1986*a*) and in red coral for spicule and axial skeleton synthesis by Allemand and Grillo (1992). As in these reports, the effect of DIDS on the calcification rate may be interpreted either as inhibition of an electrogenic Cl^- flux coupled with Ca^{2+} flux (Yasumasu *et al.* 1985) or as a decrease in the production of the carbonate moiety of $CaCO_3$ subsequent to the inhibition of HCO_3^- flux (Mitsunaga *et al.* 1986*b*; Allemand and Grillo, 1992). Further experiments are under way to investigate anion transport.

The involvement of carbonic anhydrase in biocalcification processes, including those in hermatypic corals, is well documented (Goreau, 1959; Istin and Girard, 1970; Mitsunaga *et al.* 1986*b*; Tuan *et al.* 1986; Kingsley and Watabe, 1987; Allemand and Grillo, 1992). Isa and Yamazato (1984) have shown using histochemical methods that carbonic anhydrase is localized in the calicoblastic epithelium. Our results support these studies and show that this enzyme is involved in Ca^{2+} deposition, whereas Ca^{2+} uptake into the NaOH-soluble pool appears to be insensitive to the sulphonamide tested (ethoxyzolamide).

The calcification rate is sensitive to a combination of two inhibitors of actin and tubulin polymerization, cytochalasin B and colchicin. Fujino *et al.* (1985) have previously shown that

inhibitors of tubulin assembly, colchicin and podophyllotoxin, inhibit Ca^{2+} uptake and deposition by cultured primary mesenchyme cells of echinoderms. This suggests that actin and tubulin assembly are implicated in Ca^{2+} transport within the calcifying cells. It is known that microtubules are involved in vesicular transport activity across polarized cells (see review by Schaerer *et al.* 1991). However, nothing is known about intracellular movement of molecules such as Ca^{2+}-binding proteins. While diffusion cannot be excluded, our results suggest that the cell cytoskeleton may play a role in the directed movement of these molecules.

Cellular origin of the calcium used for calcification

The post-incubation washing procedure, described here for the first time, allows examination of at least two exchangeable Ca^{2+} pools relevant to calcification in *Stylophora pistillata*. Figs 1C and 2 show that the time course of Ca^{2+} deposition displays a short lag phase of less than 2 min. A linear rate of calcification was demonstrated in the scleractinian coral *Galaxea fascicularis* by Krishnaveni *et al.* (1989), whereas a biphasic pattern was found in more slowly calcifying animals, such as echinoderms (Nauen and Böhm, 1979; Donachy and Watabe, 1986; Dafni and Erez, 1987; Lewis *et al.* 1990) or octocorals (Allemand and Grillo, 1992), where the turnover rate of compartments is much slower. A linear uptake rate indicates that no intermediate compartment exists between the external sea water and the coelenteron, thus invoking a very short diffusional pathway. In the present study, the short lag phase should correspond to transit through an intermediate cellular compartment, since our results demonstrate that Ca^{2+} must pass through cells before reaching the site of calcification (see above). The short lag phase in the calcification process suggests that the cellular Ca^{2+} compartment that supplies skeletogenic Ca^{2+} ('calcifying compartment') is rapidly equilibrated with exogenous radioactive Ca^{2+}. This means that this calcifying compartment has a rapid turnover rate or a small size or both characteristics. Our results suggest that the turnover rate of this hypothetical pool is in the region of 2 min.

What type of intracellular compartment could correspond to the calcifying compartment? The turnover rate of the NaOH-soluble pool (20 min), which anatomically corresponds to total tissue Ca^{2+}, is too slow and the pool is too large (7.12 nmol mg^{-1} protein). Furthermore, uptake of Ca^{2+} into the NaOH-soluble pool was not inhibited by Ca^{2+} channel inhibitors whereas calcification was. These results suggest that the tissue compartment identified as NaOH-soluble cannot be assumed to be the calcifying compartment. The gastrovascular pool exhibited kinetic characteristics indicative of a possible source for calcification. The very fast turnover rate of 2 min should correspond to that suggested for the calcifying compartment. However, its extracellular localization rules out its involvement as a direct source of Ca^{2+} for calcification. This leads us to hypothesize the existence of a third exchangeable Ca^{2+} compartment that our experimental approach cannot detect. This compartment should have (1) a rapid turnover rate, about 2 min, which causes it to be undetectable in the large gastrovascular pool, and (2) a small size. Ca^{2+} fluxes across this compartment should be high, 975 pmol mg^{-1} protein min^{-1} based on the calcification rate (Fig. 1C), in contrast to the flux into the tissue compartment which is only 224 pmol mg^{-1} protein min^{-1}. The bulk of skeletal Ca^{2+} should come from this compartment (Fig. 8A) which could correspond anatomically to the calicoblastic epithelium (Fig. 8B). This compartment is probably supplied directly by the gastrovascular compartment: the theoretical rate of Ca^{2+} flux through the gastrovascular compartment calculated from kinetic parameters (see Results) is 12.6 nmol mg^{-1} protein min^{-1}. This flux is 13 times larger than necessary to support the measured calcification rate (0.97 nmol mg^{-1} protein min^{-1}) and, thus, more than sufficient in capacity (Fig. 8B). Such an high flux in the gastrovascular cavity could be accomplished through the mouth by muscular pumping or by active transport through the oral epithelial cell layers as shown by Wright and Marshall (1991) in *Lobophyllia hemprichii* and *Plerogyra sinuosa*. However, since in our experiments the flux is cyanide-insensitive (Tambutté *et al.* 1995), it is possible that Ca^{2+} movement could take place across the oral tissues *via* an intercellular pathway. This was recently confirmed in our laboratory in kinetic experiments with *Heliofungia actiniformis* using an Ussing chamber. These experiments indicated that Ca^{2+} crossed the oral tissue *via* an intercellular pathway with a flux of 2.3 nmol mg^{-1} protein min^{-1}, which is higher than the calcification rate (Bénazet-Tambutté *et al.* 1996).

Compartmental analysis of Ca^{2+}

What is the nature of the NaOH-soluble Ca^{2+} pool? From an anatomical point of view, this compartment should correspond to the tissue compartment. If the cell water space is assumed to be similar in size to that this found in the sea anemone by Lopez *et al.* (1991), i.e. 2.54 μl mg^{-1} protein, it can be calculated from the Ca^{2+} compartment size (7.12 nmol Ca^{2+} mg^{-1} protein, see Table 1) that the total cellular Ca^{2+} concentration (not activity) is 2.80±0.3 mmol l^{-1}, a value typical of other cells (Carafoli, 1987). This result rules out the hypothesis of an extracellular location of this compartment since the Ca^{2+} concentration in sea water is about 10 mmol l^{-1}. However, this value should be taken with caution, since the tissues are highly heterogeneous and are made up of several cell types, including mucocytes, dinoflagellate symbionts, cnidocytes and ectodermal cells. The turnover rate of the NaOH-soluble pool is in close agreement with that found for intracellular compartments of exchangeable Ca^{2+} in other cell types (Borle, 1969*a*,*b*; Claret-Berthon *et al.* 1977). Surprisingly, Ca^{2+} channel inhibitors appeared to stimulate Ca^{2+} influx into this compartment (Fig. 4). Some authors have found that, in algae, organic channel antagonists such as nifedipine, bepridil or verapamil can increase the Ca^{2+} influx through voltage-dependent Ca^{2+} channels (reviewed by Reid and Tester, 1992). They explained this unexpected effect by an inhibition by these drugs of K^+ channels, leading to hyperpolarization. However, the absence of voltage-dependent

Ca^{2+} channels is not as unexpected in non-excitable cells (Sage *et al.* 1992).

The efflux experiments were designed to examine Ca^{2+} compartmentation further, particularly the nature of tissue compartments. The 0Ca/EGTA medium was employed to avoid the effects of isotopic dilution on specific activity during the efflux (or washing) period. Conducting the efflux on ice should reduce the redistribution of Ca^{2+} between compartments due to active transport. Comparing efflux measured in this way with efflux measured in filtered sea water, the faster components appear to correspond to similar compartments. The C1 component represents extracolonial Ca^{2+}. The kinetic characteristics of C2 and C3 are close to those found in influx experiments for the gastrovascular cavity (Tambutté *et al.* 1995) and the NaOH-soluble pool (i.e. a tissue Ca^{2+} compartment) respectively. Caution must be exercised, however, in comparing uptake kinetics under physiological conditions with efflux under different conditions.

The D600-sensitivity of the C4 component indicates the presence of voltage-dependent Ca^{2+} channels. However, this compartment exhibits a very slow rate constant (72–742 min depending on the efflux protocol, Table 2), suggesting that it is located at a deeper site within the tissue (Claret-Berthon *et al.* 1977). When efflux experiments were performed in FSW, the C4 kinetic values were not very different from those of the NaOH-soluble pool, but the C4 compartment size was considerably larger than the amount of Ca^{2+} remaining in the NaOH-soluble pool when 0Ca/EGTA was employed (Table 3). The discrepancy was not as large, but was still substantial, when both EGTA and Ca^{2+} were absent from the efflux medium. These C4 values represent compartment size at the beginning of Ca^{2+} efflux (i.e. at the end of the incubation). While this value is ultimately of greatest interest, the C4 Ca^{2+} content remaining after efflux should be similar to that recovered in the NaOH-soluble pool. The C4 Ca^{2+} content remaining after efflux was always higher (Table 3). Is all tissue Ca^{2+} recovered by the NaOH extraction? Any unrecovered Ca^{2+} would still be associated with the skeleton. The S1 component is a possible indicator of such Ca^{2+}. If one adds this amount of Ca^{2+} (Table 2) to the amount of Ca^{2+} in the NaOH-soluble pool (Table 3), the sum is consistently very close to the $C4_{180}$ Ca^{2+} value (Table 3), and a similar value is obtained in all efflux protocols except with FSW at 25 °C.

If one assumes that the C4 compartment is synonymous with a tissue compartment, then why do the apparent efflux rate constants for C4 differ between treatments, resulting in discrepancies in total C4 Ca^{2+} ($C4_0$)? It is possible that tissue Ca^{2+} or its specific activity changes during the efflux procedure. The results using the EGTA protocol suggest that skeletal Ca^{2+}, or a labile pool thereof, is being redistributed and detected in the C4 compartment. This Ca^{2+}, possibly represented by the S1 component, could be newly excreted Ca^{2+}, perhaps associated with matrix proteins but not yet deposited as $CaCO_3$.

This argument may qualify the results obtained with D600 with regard to the C4 and NaOH-soluble pools (Fig. 7); the inhibition caused by D600 may reflect differences in calcification rather than in tissue Ca^{2+} influx. When FSW is used during the efflux, there could be a decrease in cellular specific activity when unlabelled Ca^{2+} influx must be assumed to occur. The relatively slow loss of label detected from the C4 compartment (reflected in the much shorter $t_{1/2}$ values) in FSW would reflect the exchange of ^{45}Ca for unlabelled Ca^{2+} rather than unidirectional efflux of Ca^{2+}. Warmer temperatures appear to decrease the C4 (and NaOH-soluble fraction) Ca^{2+} values, and this could be due to continued operation of Ca^{2+} pumps during efflux.

The fraction of total colony Ca^{2+} uptake (sum of all fractions except C1) contributed by compartments C4, S1 and S2 is very similar in all treatments (75.5±3.3 %). Thus, all efflux protocols are similar in their ability to remove extracellular (coelenteron, etc.) Ca^{2+}, but the remaining Ca^{2+} is distributed differently. The values for Ca^{2+} content in the S2 and HCl-soluble pool were in close agreement (data not shown) for all protocols. It was clear, however, that the presence of EGTA decreased the skeletal Ca^{2+} content. Comparing the S2 or HCl-soluble values (approximately 28 nmol Ca^{2+} mg^{-1} protein h^{-1}, as determined from the values in Table 2) with calcification rates obtained using the influx protocol previously validated with the alkalinity technique (58.52 nmol Ca^{2+} mg^{-1} protein h^{-1}; Tambutté *et al.* 1995), the EGTA method provides a substantial underestimate of calcification. The results obtained in FSW at 25 °C (S2=56.3 nmol Ca^{2+} mg^{-1} protein h^{-1}, as determined from the values in Table 2) and with 0Ca/ASW (66.2 nmol Ca^{2+} mg^{-1} protein h^{-1}, as determined from the values in Table 2) appear to provide the values closest to alkalinity values.

In conclusion, we suggest that the tissues of scleractinian corals should possess two types of cells according to their sensitivity to Ca^{2+} channel inhibitors. (1) Calcium-transporting cells, which anatomically belong to the calicoblastic epithelium and have L-type voltage-dependent Ca^{2+} channels. Ca^{2+} is transported across this epithelium by an energy-consuming mechanism (Ca^{2+}-ATPase), the flux being coupled in some way to anion transport; the transcellular passage of Ca^{2+} is independent of intracellular Ca^{2+} stores, but is dependent on the cytoskeleton. (2) All other cells, which do not transport Ca^{2+} actively and which have voltage-dependent Ca^{2+} channels insensitive to the inhibitors tested or which lack this type of channel. Ca^{2+} used for building the skeleton equilibrates rapidly ($t_{1/2}$≈2–4 min) with the coelenteric compartment and with the Ca^{2+} within the Ca^{2+}-transporting cells. Thus, skeletal Ca^{2+} should cross only one epithelium (Fig. 8B). Once excreted by the calicoblastic cells, Ca^{2+} seems to exist in a transitory state, perhaps associated with the organic matrix, before being firmly deposited as $CaCO_3$. As previously concluded (Crossland and Barnes, 1977), the post-incubation procedures are critical for evaluating calcification and the compartmentation of Ca^{2+}.

The new methodologies applied in this study promise to add considerably to our knowledge of scleractinian coral

physiology. The coral microcolony eliminates many of the problems that compromised previous calcification data and limited progress in this field. Coupled with a physiological approach, the microcolony provides a model system for the systematic study of calcification and its links to other physiological processes, including zooxanthellae photosynthesis.

We thank The Marine Station of Aqaba for facilitating the collection of corals. We thank Dr Barhanin (Institut de Pharmacologie Moléculaire et Cellulaire) for his generous gift of drugs and C. Emery for his technical assistance. We also thank Dr D. Zoccola for fruitful discussions. This study was conducted as part of the OOE 1991–1995 research program. It was supported by the Council of Europe (Open Partial Agreement on Major Natural and Technological Disasters), the Programme National Récifs Coralliens (PNRCO). Support for E.M. was provided by NSF-EPSCoR (award EHR-9108761) and the OOE.

References

ADAMS, D. J. AND GAGE, P. W. (1979). Characteristics of sodium and calcium conductance changes produced by membrane depolarization in *Aplysia* neurons. *J. Physiol., Lond.* **289**, 143–161.

ALLEMAND, D., DE RENZIS, G., CIAPA, B., GIRARD, J. P. AND PAYAN, P. (1984). Characterization of valine transport in sea urchin eggs. *Biochim. biophys. Acta* **772**, 337–346.

ALLEMAND, D. AND GRILLO, M. C. (1992). Biocalcification mechanisms in gorgonians. ^{45}Ca uptake and deposition by the Mediterranean red coral *Corallium rubrum*. *J. exp. Zool.* **292**, 237–246.

BARNES, D. J. AND CHALKER, B. E. (1990). Calcification and photosynthesis in reef-building corals and algae. In *Coral Reefs* (ed. Z. Dubinsky), pp. 109–131. Amsterdam: Elsevier.

BARNES, D. J. AND CROSSLAND, C. J. (1977). Coral calcification: sources of error in radioisotope techniques. *Mar. Biol.* **42**, 119–129.

BÉNAZET-TAMBUTTÉ, S., ALLEMAND, D. AND JAUBERT, J. (1996). Permeability of the oral epithelial layers in cnidarians. *Mar. Biol.* (in press).

BILBAUT, A., HERNANDEZ-NICAISE, M. L., LEECH, C. A. AND MEECH, R. W. (1988). Membrane currents that govern smooth muscle contraction in a ctenophore. *Nature* **331**, 533–535.

BORLE, A. B. (1969*a*). Kinetic analyses of calcium movements in HeLa cell cultures. I. Calcium influx. *J. gen. Physiol.* **53**, 43–56.

BORLE, A. B. (1969*b*). Kinetic analyses of calcium movements in HeLa cell cultures. II. Calcium efflux. *J. gen. Physiol.* **53**, 57–69.

BORLE, A. B. (1990). Measurement of calcium movement across membranes: kinetic analysis and conceptualization. In *Intracellular Calcium Regulation* (ed. F. Bronner), pp. 19–75. New York: Wiley-Liss.

BOROWITZKA, M. A. (1982). Mechanisms in algal calcification. *Prog. Phycol. Res.* **1**, 137–177.

BRONNER, F. (1990). Transepithelial calcium transport in gut and kidney. In *Calcium Transport and Intracellular Calcium Homeostasis* (ed. D. Pansu and F. Bronner), pp. 199–223. Berlin: Springer-Verlag.

BUDDEMEIER, R. W. AND KINZIE, R. A. (1976). Coral growth. *Oceanogr. mar. Biol. A. Rev.* **14**, 183–225.

CABANTCHIK, Z. I. AND GREGER, R. (1992). Chemical probes for anion transporters of mammalian cell membranes. *Am. J. Physiol.* **262**, C803–C827.

CAMERON, J. N. (1990). Unusual aspects of calcium metabolism in aquatic animals. *A. Rev. Physiol.* **52**, 77–95.

CARAFOLI, E. (1987). Intracellular calcium homeostasis. *A. Rev. Biochem.* **56**, 395–433.

CHALKER, B. E. (1976). Calcium transport during skeletogenesis in hermatypic corals. *Comp. Biochem. Physiol.* **54**A, 455–459.

CHAVE, K. E., SMITH, S. V. AND ROY, K. J. (1975). Carbonate production by coral reefs. *Mar. Geol.* **12**, 123–140.

CLARET-BERTHON, B., CLARET, M. AND MAZET, J. L. (1977). Fluxes and distribution of calcium in rat liver cells: kinetic analysis and identification of pools. *J. Physiol., Lond.* **272**, 529–552.

CLAUSEN, C. D. AND ROTH, A. A. (1975). Estimation of coral growth rates from laboratory ^{45}Ca incorporation rates. *Mar. Biol.* **33**, 85–91.

CROSSLAND, C. J. AND BARNES, D. J. (1977). Calcification in the staghorn coral *Acropora acuminata*: variations in apparent skeletal incorporation of radioisotopes due to different methods of processing. *Mar. Biol.* **43**, 57–62.

DAFNI, J. AND EREZ, J. (1987). Skeletal calcification patterns in the sea urchin *Tripneustes gratilla elatensis* (Echinoidea, Regularia). I. Basic patterns. *Mar. Biol.* **95**, 275–287.

DONACHY, J. E. AND WATABE, N. (1986). Effects of salinity and calcium concentration on arm regeneration by *Ophiothrix angulata* (Echinodermata: ophiuroidea). *Mar. Biol.* **91**, 253–257.

DUBOIS, P. AND CHEN, C. P. (1989). Calcification in echinoderms. In *Echinoderm Studies*, vol. 3 (ed. M. Jangoux and J. M. Lawrence), pp. 109–178. Rotterdam: A. A. Balkema.

FUJINO, Y., MAKIHARA, R., MITSUNAGA, K. AND YASUMASU, I. (1985). Roles of cytoskeletons on spicule formation in cultured micromeres isolated from sea-urchin eggs. *Proc. 56th Annual Meeting Zool. Soc.* **2**, 945.

GLADFELTER, E. H. (1984). Skeletal development in *Acropora cervicornis*. III. A comparison of monthly rates of linear extension and calcium carbonate accretion measured over a year. *Coral Reefs* **3**, 51–57.

GOREAU, T. F. (1959). The physiology of skeleton formation in corals. I. A method for measuring the rate of calcium deposition by corals under different conditions. *Biol. Bull. mar. biol. Lab., Woods Hole* **116**, 59–75.

HAYES, R. L. AND GOREAU, N. I. (1977). Cytodynamics of coral calcification. *Proc. Third. Int. Coral Reef Symp.* **2**, 433–438.

HOSEY, M. M. AND LAZDUNSKI, M. (1988). Calcium channels: molecular pharmacology, structure and regulation. *J. Membr. Biol.* **104**, 81–105.

IP, Y. K., LIM, A. L. L. AND LIM, R. W. L. (1991). Some properties of calcium-activated adenosine triphosphatase from the hermatypic coral *Galaxea fascicularis*. *Mar. Biol.* **111**, 191–197.

ISA, Y., IKEHARA, N. AND YAMAZATO, K. (1980). Evidence for the occurrence of Ca^{2+}-dependent adenosine triphosphatase in a hermatypic coral *Acropora hebes* (Dana). *Sesoko mar. Sci. Lab. Tech. Rep.* **7**, 19–25.

ISA, Y. AND YAMAZATO, K. (1984). The distribution of carbonic anhydrase in a staghorn coral *Acropora hebes* (Dana). *Galaxea* **3**, 25–36.

ISTIN, M. AND GIRARD, J.-P. (1970). Carbonic anhydrase and mobilisation of calcium reserves in the mantle of lamellibranchs. *Calc. Tissue Res.* **5**, 247–260.

JOHNSTON, I. S. (1980). The ultrastructure of skeletogenesis in zooxanthellate corals. *Int. Rev. Cytol.* **67**, 171–214.

KINGSLEY, R. J. AND WATABE, N. (1987). Role of carbonic anhydrase in calcification in the gorgonian *Leptogorgia virgulata*. *J. exp. Zool.* **241**, 171–180.

KRISHNAVENI, P., CHOU, L. M. AND IP, Y. K. (1989). Deposition of calcium ($^{45}Ca^{2+}$) in the coral *Galeaxea fascicularis*. *Comp. Biochem. Physiol.* **94**A, 509–513.

LEWIS, C. A., EBERT, T. A. AND BOREN, M. E. (1990). Allocation of ^{45}calcium to body components of starved and fed purple sea urchins (*Strongylocentrotus purpuratus*). *Mar. Biol.* **105**, 213–222.

LOPEZ, I., EGEA, R. AND HERRERA, F. C. (1991). Are coelenterate cells permeable to large anions? *Comp. Biochem. Physiol.* **100**A, 193–198.

LOWRY, O. H., ROSEBROUGH, N. J., FARR, A. L. AND RANDALL, R. J. (1951). Protein measurement with the folin phenol reagent. *J. biol. Chem.* **193**, 265–275.

MARSHALL, W. S., BRYSON, S. E. AND WOOD, C. M. (1992). Calcium transport by isolated skin of rainbow trout. *J. exp. Biol.* **166**, 297–316.

MCCONNAUGHEY, T. (1989). Biomineralization mechanisms. In *Origin, Evolution and Modern Aspects of Biomineralization in Plants and Animals* (ed. R. E. Crick), pp. 57–73. New York: Plenum Press.

MEYRAN, J. C., GRAF, F. AND NICAISE, G. (1984). Calcium pathway through a mineralizing epithelium in the crustacean *Orchestia* in the pre-molt: ultrastructural cytochemistry and X-ray microanalysis. *Tissue & Cell* **16**, 269–286.

MILLER, R. J. AND FOX, A. P. (1990). Voltage-sensitive calcium channels. In *Intracellular Calcium Regulation* (ed. F. Bronner), pp. 97–138. New York: Wiley-Liss.

MITSUNAGA, K., AKASAKA, K., SHIMADA, H., FUJINO, Y., YASUMASU, I. AND NUMANDI, H. (1986*a*). Carbonic anhydrase activity in developing sea urchin embryos with special reference to calcification of spicules. *Cell. Differ.* **18**, 257–262.

MITSUNAGA, K., FUJINO, Y. AND YASUMASU, I. (1986*b*). Change in the activity of Cl^-, HCO_3^- ATPase in microsome fraction during early development of the sea urchin, *Hemicentrotus pulcherrimus*. *J. Biochem., Tokyo* **100**, 1607–1615.

MUELLER, E. (1984). Effects of a calcium channel blocker and an inhibitor of phosphodiesterase on calcification in *Acropora formosa*. *Proc. Advances in Reef Science, abstracts*, 87–88.

NAUEN, C. E. AND BÖHM, L. (1979). Skeletal growth in the echinoderm *Asterias rubens* L. (Asteroidea, Echinodermata) estimated by ^{45}Ca-labelling. *J. exp. mar. Biol. Ecol.* **38**, 261–269.

NEUFELD, D. S. AND CAMERON, J. N. (1994). Effect of the external concentration of calcium on the postmoult uptake of calcium in blue crabs (*Callinectes sapidus*). *J. exp. Biol.* **188**, 1–9.

PIETROBON, D., DI VIRGILIO, F. AND POZZAN, T. (1990). Structural and functional aspects of calcium homeostasis in eukaryotic cells. *Eur. J. Biochem.* **193**, 599–622.

REID, R. J. AND TESTER, M. (1992). Measurements of Ca^{2+} fluxes in intact plant cells. *Phil. Trans. R. Soc. Lond. B* **338**, 73–82.

ROER, R. D. (1980). Mechanisms of resorption and deposition of calcium in the carapace of the crab *Carcinus maenas*. *J. exp. Biol.* **88**, 205–218.

SAGE, S. O., MAHAUT-SMITH, M. P. AND RINK, T. J. (1992). Calcium entry in non excitable cells: lessons from human platelets. *News physiol. Sci.* **7**, 108–113.

SCHAERER, E., NEUTRA, M. R. AND KRAEHENBUHL, J. P. (1991). Molecular and cellular mechanisms involved in transepithelial transport. *J. Membr. Biol.* **123**, 93–104.

SCHMIDT, T., PATTON, C. AND EPEL, D. (1982). Is there a role for the Ca^{2+} influx during fertilization of the sea urchin egg? *Dev. Biol.* **90**, 284–290.

SILVERTON, S. F. (1991). Carbonic anhydrase and skeletogenesis. In *The Carbonic Anhydrases. Cellular Physiology and Molecular Genetics* (ed. S. J. Dodgson, R. E. Tashian, G. Gros and N. D. Carter), pp. 357–363. New York: Plenum Press.

SIMKISS, K. (1976). Cellular aspects of calcification. In *The Mechanisms of Mineralization in the Invertebrates and Plants* (ed. N. Watabe and K. M. Wilbur), pp. 1–32. Columbia, SC: University of South Carolina Press.

SIMKISS, K. AND WILBUR, K. M. (1989). *Biomineralization: Cell Biology and Mineral Deposition.* New York: Academic Press.

SPEDDING, M. AND PAOLETTI, R. (1992). Classification of calcium channels and the sites of action of drugs modifying channel function. *Pharmac. Rev.* **44**, 363–376.

TAMBUTTÉ, E., ALLEMAND, D., BOURGE, I., GATTUSO, J.-P. AND JAUBERT, J. (1995). An improved ^{45}Ca protocol for investigating physiological mechanisms in coral calcification. *Mar. Biol.* **122**, 453–459.

TUAN, R. S., CARSON, M. J., JOZEFIAK, J. A., KNOWLES, K. A. AND SHOTWELL, B. A. (1986). Calcium-transport function of the chick embryonic chorioallantoic membrane. I. *In vivo* and *in vitro* characterization. *J. Cell Sci.* **82**, 73–84.

VAN BREEMEN, C., AARONSON, P. AND LOUTZENHISER, R. (1979). Na^+, Ca^{2+} interactions in mammalian smooth muscle. *Pharmac. Rev.* **30**, 167–208.

WHEELER, A. P. (1992). Mechanisms of molluscan shell formation. In *Calcification in Biological Systems* (ed. E. Bonucci), pp. 179–216. Boca Raton: CRC Press.

WICTOME, M., HENDERSON, I., LEE, A. G. AND EAST, J. M. (1992). Mechanism of inhibition of the calcium pump of sarcoplasmic reticulum by thapsigargin. *Biochem. J.* **283**, 525–536.

WILBUR, K. M. (1976). Recent studies of invertebrate mineralization. In *The Mechanism of Mineralization in the Invertebrates and Plants* (ed. N. Watabe and K. Wilbur), pp. 79–108. Columbia, SC: University of South Carolina Press.

WILBUR, K. M. AND SIMKISS, K. (1979). Carbonate turnover and deposition by metazoa. In *Studies in Environmental Sciences – Biochemical Cycling of Mineral-forming Elements*, vol. 3 (ed. P. A. Trudinger and D. J. Swaine), pp. 69–106. Amsterdam: Elsevier.

WRIGHT, O. P. AND MARSHALL, A. T. (1991). Calcium transport across the isolated oral epithelium of scleractinian corals. *Coral Reefs* **10**, 37–40.

YASUMASU, I., MITSUNAGA, K. AND FUJINO, Y. (1985). Mechanism for electrosilent Ca^{2+} transport to cause calcification of spicules in sea urchin embryos. *Expl Cell Res.* **159**, 80–90.